

1 **Modelling forest lines and forest distribution patterns with remote sensing data in a**
2 **mountainous region of semi-arid Central Asia.**

3

4 Michael Klinge¹⁾, Jürgen Böhner²⁾, Stefan Erasmi¹⁾

5

6 ¹⁾Institute of Geography, University of Göttingen, Goldschmidtstr. 5, D-37077 Göttingen, Germany,
7 mklingle1@gwdg.de

8 ²⁾Institute of Geography, University of Hamburg, Bundesstraße 55, D-20146 Hamburg, Germany,
9 boehner@geowiss.uni-hamburg.de

10

11 Correspondence to: M. Klinge (mklingle1@gwdg.de)

12

13 **Abstract**

14 Satellite images and digital elevation models provide an excellent database to analyse forest
15 distribution patterns and forest limits in the mountain regions of semi-arid Central Asia at the regional
16 scale. For the investigation area in the northern Tien Shan a strong relationship between forest
17 distribution and climate conditions could be found. Additionally areas of potential human impact on
18 forested areas are identified at lower elevations near the mountain border based on an analysis of the
19 differences of climatic preconditions and present occurrence of forest stands.

20 The distribution of spruce (*Picea schrenkiana*) forests is hydrologically limited by a minimum annual
21 precipitation of 250 mm and thermally by a minimum monthly mean temperature of 5 °C during the
22 growing season. While the actual lower forest limit increases from 1,600 m asl (above sea level) in the
23 northwest to 2,600 m asl in the southeast, the upper forest limit rises in the same direction from 1,800
24 m asl to 2,900 m asl. In accordance with the main wind directions, the steepest gradient of both forest
25 lines and the greatest local vertical extent of the forest belt of 500 to 600 m and maximum 900 m
26 occur at the northern and western mountain fronts.

27 The forests in the investigation area are strongly restricted to north facing-slopes, which is a common
28 feature in semi-arid Central Asia. Based on the presumption that variations in local climate conditions
29 are a function of topography, the potential forest extent was analysed with regard to the parameters
30 slope, aspect, solar radiation input and elevation. All four parameters showed a strong relationship to
31 forest distribution, yielding a total potential forest area that is 3.5 times larger than the present forest
32 remains of 502 km².

33

1 **1 Introduction**

2 The latitudinal and elevational variation of distinct plant associations and geomorphologic landscape
3 units has been used for a long-time to deduce regional environmental and climatical conditions in
4 geosciences (e.g. Humboldt, 1845-1862; Troll, 1973a, b; Hövermann, 1985). Image classification and
5 GIS-modelling of remote sensing data are standard methods to map landscape elements and their
6 distribution in remote areas, which are poorly accessible due to logistic or political difficulties.
7 Satellite analysis based on automated image processing offers a quick and beneficial alternative to
8 field mapping or manual digitalisation from aerial image (Mayer and Bussemer, 2001). While satellite
9 images like Landsat data provide excellent information to delineate the spatial forest distribution
10 (Hansen et al., 2013), SRTM (Shuttle Radar Topography Mission) data can be used to examine relief
11 dependent distribution patterns with a digital terrain model (DTM). The combination of these two data
12 sets enables high resolution mapping at regional to local scale.

13 The geocologic and climatic environmental settings control the natural distribution of forest stands
14 (Holtmeier, 2000; Körner, 2012; Miede et al., 2003). In addition, the actual situation can strongly be
15 influenced by human activities like logging, fire clearing and animal grazing, which decreases the
16 potential natural forest area (PFA). This often makes it difficult to differentiate between natural factors
17 and human impact on the distribution of timbered areas. In general, human activity has reduced the
18 forest area since prehistorical times so that the actual forest area (AFA) pattern mostly represent the
19 minimum of the potential environmental distribution range. However, due to the possibility of
20 anthropogenic forest management and afforestation during the last centuries forests may occur at sites
21 less favourable for natural tree growth.

22 Due to the highly continental, cold and semi-arid climate in Central Asia, tree growth is mostly
23 determined by topography parameters. Forest stands beyond groundwater favoured sites are
24 predominantly limited to north-facing slopes in the mountains with an upper and lower forest limit
25 (Dulamsuren et al., 2014; Hilbig, 1995; Klinge et al., 2003; Treter, 1996, 2000).

26 Different definitions have been used for tree- and forest lines (Körner, 2012; Körner and Paulsen,
27 2004). The treeline ecotone covers three main boundary lines at the upper limit of forest distribution.
28 The highest is the tree species line, where tree seedlings occur but no adult trees. The treeline is the
29 maximum elevation where patches of forest can exist at topographic favoured places. In our
30 investigation we refer to the forest line, which is defined as the limit of closed forest at the upper
31 (timberline) and lower boundary of forest distribution.

32 For the region of northern Tien Shan in China, Dai et al. (2013) state an upper forest line beginning
33 with 2,900 m asl in the west, which decreases eastward down to 2,500 m asl and then rises again to
34 2,900 m asl in the east. In the north-western Tien Shan Fickert (1998) reports an upper forest line of
35 2,900 and 2,850 m asl and a lower forest line of 2,400 m and 2,500 m asl, respectively for the
36 Sailijski-Alatau and Kungeij-Alatau. In the Altai Mountains Klinge et al. (2003) found upper forest

1 lines increasing eastward from 1,800 m asl to 2,600 m asl and lower forest lines concurrently
2 increasing from 1,000 m asl to 2,200 m asl while the vertical extension of the forest belt varies
3 between 400 and 1,200 m.

4 Tree growth in high mountains is generally restricted by temperature conditions (Haase et al., 1964;
5 Holtmeier, 2000; Jobbagy and Jackson, 2000; Körner, 2012). The upper forest line is a thermally
6 determined distribution boundary that is generally defined by the mean July temperature (Walter and
7 Breckle, 1994) or the warmest month isotherm of 10 °C. According to Körner (2012) and Körner and
8 Paulsen (2004) this parameter is not suitable in all parts of the world. This can be seen in Fickert
9 (1998), who shows that the upper forest line in the northern Tien Shan coincides well with the 10 °C
10 July-isotherm, while further south in NW-Himalaya and NW-Karakorum it is connected to the July-
11 isotherms of 16 °C and 12 °C, respectively. For the eastern side of the northern Tien Shan Dai et al.
12 (2013) report a mean temperature of the warmest month of 10.5 °C at the mean position of the alpine
13 forest line. Also the mean annual air temperature (MAAT) is weakly correlated to the forest line
14 because it includes temperatures from the non-growing season which play a minor role for tree growth
15 (Jobbagy and Jackson, 2000; Körner, 2012).

16 A suitable way to describe the temperature environment at the upper forest line is a minimum
17 threshold value for the mean air temperature during the growing season which is defined as the period
18 of monthly mean temperatures above 5 °C (Dai et al., 2013; Körner, 2012; Körner and Paulsen, 2004).
19 Based on the strong correlation between soil and air temperatures, Körner and Paulsen (2004) state a
20 global range of 5.5 to 7.5 °C for minimum mean air temperature during the growing season. Paulsen
21 and Körner (2014) developed a climate-based model for treeline prediction by defining the growing
22 season as days with mean temperature above 0.9 °C and a mean temperature of more than 6.4 °C
23 during that time. For the upper forest line between 2,750 and 2,920 m asl in the Tien Shan Mountains
24 in Kyrgyzstan Körner (2012) found a mean temperature of 6.5 °C during the 155 days of the growing
25 season (late April until late September).

26 The forest expansion into dry regions is controlled by precipitation and soil water supply (Dulamsuren
27 et al., 2010, 2014; Kastner, 2000; Klinge et al., 2003). Between the more humid mountain regions and
28 the arid basins of Central Asia a lower limit of forest distribution occurs which is termed the lower
29 forest line. According to Walter and Breckle (1994) this forest distribution boundary coincides with an
30 annual precipitation of at least 300 mm, while Holdridge (1947) proposes 250 mm and Miehe et al.
31 (2003) found *Juniperus* trees in southern Tibet growing in regions with annual precipitation between
32 200 and 250 mm. Dulamsuren et al. (2010) state an annual precipitation between 230 and 400 mm at
33 lower elevations for larch forests in northern and central Mongolia. In western Mongolia Dulamsuren
34 et al. (2014) found coniferous forests existing at annual precipitation near 120 mm, which are
35 explained by soil water benefits due to the occurrence of permafrost ice in the soil.

1 Everywhere in mountainous areas of the semi-arid Inner Asian forest-steppe coniferous forests are
2 restricted to north facing slopes. While the north-facing slopes are dominated by larch trees (*Larix*
3 *sibirica*) in Mongolia, spruce trees (*Picea schrenkiana*) occur in the Tien Shan Mountains (Dai et al.,
4 2013; Fickert, 1998; Liu et al., 2013; Wang 2005, 2006). Thus the restriction of conifers to north-
5 facing slopes in the Inner Asian forest-steppe is not bound to certain tree species but rather to the
6 environmental settings.

7 The semi-arid climate conditions generate an overall deficiency of moisture which considerably
8 influences the elevational forest distribution and may even control the upper forest limit (Liang et al.,
9 2012; Liu et al., 2013; Miede et al., 2008). A specific relief position is combined with particular
10 climate conditions like temperature, precipitation, evaporation and insulation, which are similar at
11 comparable sites in the surroundings. For this reason the relief parameters elevation, aspect, slope
12 angle and solar radiation input can be used to define topoclimatic conditions in mountain regions
13 (Miede et al., 2003). However, to identify potential forest sites based on those definitions, the geologic
14 and soil properties have to be comparable.

15 The impact of human activity on vegetation and especially on the forest since prehistorical times is a
16 permanent question that needs to be proofed to clarify the environmental significance of any actual
17 forest line (Miede and Miede, 2000). Dulamsuren et al. (2014) found a considerable anthropo-
18 zoogenic influence on the actual lower forest line in the Mongolian Altai. For northern Mongolia
19 Schlütz et al. (2008) showed that the present vegetation pattern in the mountain taiga where steppes
20 occur on south-facing slopes is caused by climate conditions and relief, and is not originating from
21 human activities.

22 Human impact on natural forests in Kazakhstan goes back to prehistoric times with nomadism and
23 animal grazing as lifestyle adapted to the natural framework of the steppe (Karger, 1965; Giese, 1981,
24 1983). During summertime the alpine meadows and mountain steppes in the upper mountains were
25 regularly used as pastures for the livestock. Even during Soviet times in Kazakhstan the nomadic
26 movements were generally adopted by the Sowchos-System. Even today the alpine pastures are still in
27 use. Extensive animal grazing prohibits the rejuvenation of trees and nomads may expand the
28 grassland by fire setting.

29 Spatial models, which are able to predict the climatically induced forest distribution and especially the
30 upper forest line on a global scale by exclusively using spatial climate data already exist (Paulsen and
31 Körner, 2014). However, a clear method to empirically distinguish the actual forest distribution and its
32 elevational limits for small areas covering a single mountain system and to simultaneously proof the
33 potential human impact is lacking. In this investigation we introduce a procedure to solve this problem
34 based on medium resolution remote sensing data. In addition, spatially explicit climate data and tree
35 growth limiting climate parameters serve to differentiate potential human impact from natural
36 conditions in the forest distribution.

1 **2 Study Area**

2 The detailed investigation area Uzynkara ridge or Ketmen mountain range is located in the
3 northernmost part of the Tien Shan Mountains in Central Asia at the border between Kazakhstan and
4 China (79° - 81° E / $42^{\circ}45'$ - $43^{\circ}45'$ N) (Fig. 1). This closed mountain system was chosen for
5 investigation because it provides excellent topographic preconditions to clearly indicate the lower and
6 upper boundaries of forest distribution between the middle and central part of Asia. It is filling a gap
7 of information about forest lines between regions of the Tien Shan mountains in the south and east,
8 and the Altai mountains in the north (Fickert, 1998; Dai et al., 2013; Klinge et al., 2003). The main
9 cities in the region are Shonzy and Kegen. The complete mountain range is part of the catchment area
10 (CA) of the Ili river in the north. While the northern mountain side is directly drained to the Ili river,
11 the Kegen river in the southern intermountain basin first flows westward and then turns as Sharyn
12 river into a northern direction, and the Tekes river in the southernmost part runs eastward to Chinese
13 territory. The mountain system is structured by two main ridges, a northern front range (NFR) and a
14 southern mountain range (SMR), which converge in the east and enclose an intermountain basin in the
15 west. The highest peak is the Nebesnaja reaching 3,652 m asl. A high mountain plateau in \sim 3,400 m
16 asl is dropping southward, while the north facing slopes are cut steeply by Pleistocene cirques. Today,
17 no glaciation but permafrost occurs in the uppermost areas.

18 The mountain border is tectonically clearly accentuated against the alluvial fans and fanglomerats in
19 approximately 1,500 m asl in the North and in 2,000 m asl in the southern intermountain basin
20 following west to east trending fault lines. The mountains mainly consist of metamorphic and volcanic
21 Carboniferous and Devonian rocks including several Palaeozoic granite bodies. Locally also Permian,
22 Silurian and Jurassic rocks are distributed.

23 The MAAT in Almaty (848 m asl) is 8.7° C and in Karakol (1,744 m asl) which is situated south of
24 the investigation area 6.3° C, respectively (Fickert, 1998). According to Medeu (2010) the mean air
25 temperature is between -8 and -10° C in January and between 20 and 24° C in July. In wintertime the
26 Siberian anticyclone produces weather conditions with cold air masses in the basins and warmer air
27 temperatures above the inversion layer between 1,000 and 1,550 m asl (Giese, 1973).

28 The majority of precipitation in Kazakhstan comes along with air masses from western and south-
29 western directions. In the mountains of northern Tien Shan mainly convective rainfall occurs in spring
30 and autumn. Additionally cold air masses from northern directions bring precipitation to the northern
31 Tien Shan in summertime (Böhner, 2006; Lydolph, 1977). According to Giese (1973) the annual
32 precipitation in the basins of the foreland lies between 100 and 300 mm, in the lower mountains and in
33 the intermountain basin it is between 300 and 400 mm. In the mountains it increases to more than 800
34 mm. The precipitation maxima occur in May, June, and with minor secondary maximum in
35 September.

1 The foreland, basins, and treeless mountain areas are covered by steppe vegetation with forb and
2 bunch grass (Medeu, 2010). To the drier regions in the north it changes to grassland, sagebrush desert,
3 saltwort, and sedge vegetation. The forest belt mainly consists of spruce trees (*Picea schrenkiana*). In
4 the westernmost part aspen trees (*Populus tremula*) and in the northeastern part birch trees (*Betula*
5 *pendula*) additionally occur. On the southern slopes shrub areas exist also.

6 The soils are distributed according to the climate conditions and the vegetation zones (Medeu, 2010).
7 In the foreland desert soils occur. In the lower front ranges and in the intermountain basin mountain
8 steppe soils of castanozem and chernozem type are distributed. In the forest belt dark chernozems
9 which are locally bleached and podzolized occur under forest and pheaozem soils exist at meadow
10 steppe sites. In the high elevations alpine and subalpine soils occur with mountain meadows and
11 meadow steppes.

12 Arable land in eastern Kazakhstan is located in front of the mountain ranges on the alluvial fans in the
13 basins and on the foothills in lower elevation. In this transition zone between the pediments and
14 mountain ranges the soils are improved by a content of Pleistocene loess (Giese, 1983; Karger, 1965;
15 Machalett et al., 2006). In front of the mountain border, the rivers spend the water for irrigation
16 cultivation on the pediments. On the foothills agriculture is supported by sufficient rainfall as the so-
17 called “Bogar”-Cultivation (Giese, 1983). According to these requirements the settlements are located
18 along main valleys at the mountain boundary. Around the settlements wood-cutting is pronounced for
19 construction and fuel.

20 **3 Methods**

21 A schematic workflow of the GIS-analysis procedure with input data, intermediate data, and output
22 data is presented in Fig. 2. The analysis is divided into two main processes: The first is working on the
23 relief parameters to estimate the PFA and the second conducts the delineation of the upper and lower
24 forest lines. The forest lines are defined as the distribution boundaries of closed forest stands with
25 areas larger than 0.5 ha, disregarding single trees which may represent special environmental places or
26 remnants of former forests. Trees near the rivers of the valley bottoms were excluded from the
27 examination because these are groundwater favoured sites which are mostly occupied by deciduous
28 trees.

29 The determination of the AFA in the investigation area was achieved based on a supervised maximum
30 likelihood classification from multispectral satellite images (visible light and infrared channels) of
31 Landsat 7/ETM+ of the 13th September 2000 (Fig. 3). Aerial photos provided as imagery and Bing
32 basemaps by ESRI served for the detection of forest area reference sites for training and validation of
33 the classifier. Two classes were built and manually digitised for the classification and validation
34 process. One class represents the forest areas and the other class includes different kinds of no forest
35 landscape. Depending on the ground resolution of 30 x 30 m one pixel covers the occurrence of
36 several individual trees so that small clearings and aisles could have been disregarded. The confusion

1 matrix in Table 1 shows a producer's accuracy of 89% for forest areas, where ~6% of the forest area
2 were used for validation. This possible underestimation of the forest area of up to 11% mainly occurs
3 at the borders of closed forest, where the classification depends on the quantity of trees inside of one
4 Landsat pixel.

5 The relief parameters elevation, aspect, slope gradient, and total solar radiation input were derived
6 from a DTM based on SRTM-data (Rabus et al., 2003), which was converted to UTM-zone 44 North
7 with a spatial resolution of 90 x 90 m. The polygons of the delineated forest stands were intersected
8 with the relief parameters in order to investigate the relief dependent spatial distribution of forest sites
9 in the study area. In addition, the statistics of all relief parameters were computed for the total study
10 area (TSA) to indicate the potential impact of topography on the spatial distribution of forest stands
11 (Fig. 4). The PFA was then identified based on the assumption of confidence ranges for all four relief
12 parameters, which were found responsible for forest distribution. This range was defined by the
13 standard deviation (95% confidence interval) from single frequency distribution of the relief
14 parameters aspect, slope gradient, and sum of solar radiation input during the mean growing season
15 (March to November). While these parameters are not systematically influenced by human impact, the
16 vertical distribution may have been changed by forest clearing at the lower and upper boundary.
17 Therefore 99% of the frequency distribution of the elevation parameter was chosen in this case.

18 Baseline climate data sets for Central Asia, comprising monthly radiation, temperature and
19 precipitation data in a horizontal resolution of 0.5 arc seconds (approximately 1,200 m in longitudinal
20 and 850 m in latitudinal direction) are provided by Böhner (2006). The regular-grid climate layers
21 were estimated using an empirical modelling approach, which basically integrates statistical
22 downscaling of coarse resolution atmospheric fields (NCAR / NCEP-CDAS reanalyses series)
23 (National Center for Atmospheric Research / (National Center for Environmental Prediction - Climate
24 data assimilation system, Kalnay et al., 1996) and GIS based surface parameterization techniques, to
25 sufficiently account for the topographic heterogeneity of the target area. A comprehensive description
26 of data bases and modelling techniques is given in Böhner (2006) and Böhner and Antonic (2009).
27 The suitability and precision of the modelling approach is discussed in Gerlitz et al. (2013, 2014) and
28 Soria-Auza et al. (2010).

29 The frequency distribution of selected climate parameters related to the AFA and the TSA shown in
30 Fig. 5 was calculated in the same way as described above. In contrast to the high resolution of the
31 SRTM-data the climate data has a resolution about 10 times lower which leads to a generalisation and
32 coarser scale of relief positions, where climatic differences between slope aspects inside the valleys
33 are averaged. The climate data related to the forest stands is analysed by the climatic limitation values
34 for forest development to detect potential human impact on the forest distribution patterns when
35 obvious discrepancies occur.

1 To outline the actual forest lines it is initially necessary to segment the relief into small CAs, which
2 represent small side-valleys or slope niches divided by convex ridges. This is done by computing the
3 surficial hydrology regime from the DTM. The size of a CA is given by the threshold value for the
4 stream definition function, which assigns the minimum number of cells to discharge into a specific cell
5 to start a depth contour. In this study a value of 200 was found practical for the lower forest line and a
6 value of 100 was suitable for the upper forest line. The single CAs generally consist of a part from the
7 left and right side of a valley. Having different aspects in one segment is expedient to receive a general
8 forest line value for one valley section.

9 After combining the catchment polygons with the forest polygons it is possible to determine the
10 maximum and minimum elevation values for forests inside a single CA. The calculated values are
11 spatially allocated as points to the position of those pixels which have the determined forest line value.
12 To eliminate the preconditions on the lower forest line given by the elevation limits of the relief only
13 those minimum values of forest stands were chosen, which are more than 50 m higher as the total
14 minimum value of the CA. The distance between the highest forest stands and the crest line above has
15 a special influence on the upper forest line which is called the “summit syndrome” by Körner (2012).
16 Near the summits the local climate conditions strongly suppress tree growth by stronger wind, reduced
17 temperature and snow drift. To receive a reasonable value for the climatic upper forest line and to
18 eliminate preconditions by relief height, only those maximum forest values were chosen which lie
19 more than 100 m below the total maximum elevation of the catchment. Finally, the forest lines were
20 calculated from the remaining points by a natural neighbour interpolation method.

21 **4 Results**

22 **4.1 Relief parameterisation**

23 The total AFA in the investigation area is 502 km² (Fig. 3). Frequency distributions of relief
24 parameters for the AFA are shown in Fig. 4. The slope gradient and solar radiation of the forest stands
25 show a normal distribution. The values with maximum distribution are 28° for slope gradient and
26 1,075 kWh/m² for the sum of solar radiation input (Table 2). Less than 5% of the forests exist on
27 southern slopes (SE-S-SW). The curve of the parameter aspect has a steeper left slope and a maximum
28 value in the north-western direction (315°), which is strongly related to the diurnal air temperature
29 trend caused by insolation and heating processes on different slope directions. This underlines the fact
30 that the strong relation of forest distribution to slope aspect is caused by natural environmental
31 conditions. Nomads and woodcutters approach to forest transformation by logistic problems of access
32 in the relief, which reduces the pure signal of elevation in the data. Climate controls environmental
33 conditions in a coarser regional scale and is creating sharper elevational boundaries. The curve of the
34 parameter elevation has a shallow left and a steep right slope, which indicates human impact on forest
35 distribution at the lower boundary. The lower forest lines start at 1,575 m asl and the upper forest lines

1 exceed 2,900 m asl so that the maximal vertical distance of the forest limits for the entire investigation
2 area is 1,325 m (Table 2).

3 The TSA as equal positions for forests in the mountain area were inferred from the forest lines and
4 represent the total elevation belt from 1,500 and 2,900 m asl. Except for the slope gradient diagram,
5 the flat slope positions $<5^\circ$ were additionally excluded from the TSA. The resulting TSA area is
6 approximately 4,975 km². In regard to the independent frequency distribution curves of the relief
7 parameters in Fig. 4 between forest stands and the total TSA no statistical influence of the main
8 topographic pattern on the forest distribution is detectable.

9 From the statistical point of view all four relief parameters control the forest distribution. Therefore, it
10 is necessary to check the modelling accuracy of the PFA received from one single relief parameter
11 against the combination of all four relief parameters (Table 3). Comparing the modelled PFA and the
12 AFA four different classes can be built: 1.) PFA with AFA and 2.) no PFA without AFA are
13 representing the mapped situation, 3.) PFA without AFA, and 4.) no PFA with AFA are representing
14 the differences between modelling and mapping. To receive a statistical background for the evaluation
15 of the modelling quality of the delineated PFA, it is once related to the sum (FA_{AP}) of AFA and the
16 PFA and twice referred to the total mountain area (TMA) of 8,126 km², when the mountain boundary
17 to the pediments of the foreland is generally defined by the changeover line of the slope gradient at
18 2.5°. From all four single relief parameters the modelling based on the slope aspect coincides best with
19 the actual situation, but anyway the combination of all four parameters obviously enhances the
20 prediction accuracy (Table 3). The PFA calculated from all 4 relief parameters is 1,825 km² and
21 therefore 3.5 times larger than the AFA. Fig. 3 shows the spatial differences between the AFA and
22 PFA. In relation to the AFA the PFA generally extends to the lower and upper elevations.

23 **4.2 Forest line patterns**

24 Fig. 6 shows the lower forest line in the investigation area starting at 1,600 m asl in the northwest and
25 increasing to 2,600 m asl in the southeast. Values for the lower forest line mostly are derived from the
26 lower CAs but there are also many CAs in the higher elevations of the NFR, where the forest stands do
27 not reach the valley bottom. This phenomenon may be caused by the local relief of tree free flat valley
28 bottoms, which would be rather a climate than a topographic signal. But regarding the lower forest line
29 in the second mountain range southeast of the intermountain basin and behind the NFR the lower
30 forest line remains at a higher elevation around 2,400 m asl. Here the high lower forest line position is
31 obviously caused by the drier conditions of the rain shadow position, which may also be true for the
32 upper valleys in the NFR.

33 The upper forest line distribution and the area above the forest line are shown in Fig. 7. In the NFR the
34 upper forest line at the mountain border starts in 1,800 m asl in the west and increases to 2,200 m asl
35 in the east maintaining a vertical distance of 200 m to the lower forest line. From the mountain border
36 in the north to the crest line the upper forest line rises to 2,800 m asl and crossing the intermountain

1 basin it lies in an elevation between 2,400 and 2,800 m asl in the SMR. The local vertical distance of
2 the forest belt reaches its maximum value of more than 900 m at the northern side of the NFR. On the
3 southern side and in the SMR the forest belt is very narrow with vertical distances between 50 and 400
4 m.

5 **4.3 Climate environmental conditions**

6 The environmental conditions were analysed in terms of frequency distribution of climate parameters
7 for the AFA (Fig. 5) and were mapped together with the AFA (Fig. 8-10). The diagrams in Fig. 5
8 show the differences between AFA and TSA for all climate parameters except for the MAAT, which
9 was already excluded as significant forest limitation parameter.

10 The lowest value class of forest stands for annual precipitation is 250 mm, while the highest potential
11 evapotranspiration is up to 1,100 mm/a.. One third of the AFA lies in areas with a negative potential
12 water balance (pWB, i.e. the difference between annual precipitation and potential evapotranspiration,
13 cf. Fig. 5) but with a precipitation amount between 300 and 700 mm/a (Fig. 8). These areas are
14 specially situated at the westernmost edges and on the southern slopes of the mountain ranges. While
15 the westernmost sites are exposed to the westerlies which transport most of the humidity, the southern
16 slopes lie in the rain shadow but at a higher elevation and therefore the lower forest line is around 600
17 m higher than on the northern side of the NFR.

18 In the eastern part of the northern side of the NFR the AFA belt is very small and concurrently the
19 lower forest line increases to 2,000 m asl, 400 m higher than in the western part of the NFR. Here the
20 lower forest line occurs at precipitation of 700 mm and at positive pWB of 150 to 300 mm/a, while the
21 PFA extends more into the lower slope positions which corresponds to the mean values of the regions
22 described above. This is an indication for a non-natural distribution and points to greater human
23 influence on forests in this region.

24 The forest distribution related to mean air temperature in July ranges between 7 and 17 °C, with a
25 maximum around 11 to 12 °C (Fig. 5). Comparing the AFA and PFA with the July-isotherms (Fig. 9),
26 shows that the upper AFA is mainly bordered by the 10 °C July-isotherm, but also extends to the 8 °C
27 July-isotherm at many places. The upper PFA is generally aligned to the 8 °C July-isotherm. Fig. 10
28 shows the distribution of the monthly mean air temperature 5 °C isotherm during the growing season
29 and the AFA. Except at the westernmost part the 5 °C isotherm is above the AFA between June and
30 September and the upper AFA boundary coincides well with the 5 °C isotherm of September. The
31 PFA at the upper forest boundary extends up to the position of 5 °C isotherm in June, where the
32 growing season obviously becomes very short at these high elevated places. As shown in Fig. 9 and 10
33 the PFA at the upper limit is overestimated and the upper AFA boundary generally has a natural
34 limitation.

35 **5 Discussion and conclusions**

1 It was shown that the AFA and the forest lines coincide well with the local climate conditions. At the
2 lower limit forests are restricted to a minimum annual precipitation of 250 mm. The upper forest line
3 is combined to the 10 °C July-isotherm in most places and to the minimum monthly mean temperature
4 of 5 °C for the period between June and September. In the more humid parts of the investigation area
5 at the western and northern slopes of the NFR both forest lines have a steep gradient and the forest belt
6 has its greatest vertical extension between 500 and 600 m and locally up to 900 m. This fits well to the
7 findings of increasing vertical forest extension concurrent with increasing humidity and vice versa by
8 Fickert (1998), Dai et al. (2013), and Klinge et al. (2003) in the surrounding regions. Besides
9 temperature, rainfall influences the upper forest line because clouds reduce the air temperature by
10 shadowing and reflection of solar insolation. This is explaining the steep gradient of the upper forest
11 line at the windward side of the mountain ridges.

12 The comparison of the AFA with climate data reveals a strong relation between the distribution
13 patterns at the upper boundary but divergences occur at the lower boundary. This indicates human
14 impact on the forests at the mountain borders modifying the lower forest line, while the upper forest
15 line represents the natural condition. Accordingly the PFA derived from relief parameters at lower
16 elevations indicates additional area for more potential natural forest. The PFA at the upper boundary is
17 overestimated by highest forest stands occurring at few climate favoured places, because we used the
18 total vertical distance of forest distribution as a relief parameter instead of the standard variation
19 presuming that extensive logging may also occur in the alpine meadow pastures. GIS-analysis
20 combined with multispectral satellite images and DTM is well suited to determine forest lines and
21 potential forest areas for semi-arid regions in a local to regional scale. For forest line delineation it is
22 necessary to eliminate elevation values which are restricted by the relief conditions and do not
23 represent climatic limitations. DTM-derived relief parameters slope aspect, gradient and solar
24 radiation serve well as indicators for the climatic environment in the investigation area and help to
25 transfer environmental settings to other places in the broader study area. Human impact is recognized
26 by the evaluation of the parameter elevation. Therefore a forest line evaluation with respect to the
27 general climatic conditions has to be performed before the parameter elevation is incorporated into the
28 spatial delineation process of the PFA. In conclusion, the proposed workflow is a helpful method for
29 the evaluation of the potential forest distribution and the delineation of human impact. It can be used
30 to indicate local climate variability, for landscape analysis and for effective reforestation planning.

31 **Acknowledgements**

32 The authors would like to thank the U.S. Geological Survey for making the satellite data free available
33 for scientific research. We acknowledge support by the Open Access Publication Funds of the
34 Goettingen University. We also thank Prof. Lehmkuhl and two anonymous referees for their great
35 support to improve the manuscript of this publication.

36

1 **References**

- 2 Böhner, J.: General climatic controls and topoclimatic variations of Central and High Mountain Asia,
3 *Boreas*, 35, 279-295, 2006.
- 4 Böhner, J. and Antonic, O: Land-Surface Parameters Specific to Topo-Climatology, in: Hengl, T. and
5 Reuter, H.I. [Eds.]: *Geomorphometry: Concepts, Software, Applications*, Dev. Soil Science, 33, 195-
6 226, 2009.
- 7 Dai, L., Li, Y., Luo, G., Xu, W., Lu, L., Li, C., and Feng, Y.: The spatial variation of alpine
8 timberlines and their biogeographical characteristics in the northern Tianshan Mountains of China,
9 *Environ. Earth Science*, 68, 129–137, doi 10.1007/s12665-012-1721-0, 2013.
- 10 Dulamsuren, C., Hauck, M., Khishigjargal, M., Leuschner, H. H., and Leuschner, C.: Diverging
11 climate trends in Mongolian taiga forests influence growth and regeneration of *Larix sibirica*,
12 *Oecologia*, 63, 1091–1102, doi 10.1007/s00442-010-1689-y, 2010.
- 13 Dulamsuren, C., Khishigjargal, M., Leuschner, C., and Hauck, M.: Response of tree-ring width to
14 climate warming and selective logging in larch forests of the Mongolian Altai, *J. Plant Ecol.*, 7, 24-38,
15 doi 10.1093/jpe/rtt019, 2014.
- 16 Fickert, T.: Vergleichende Beobachtungen zu Solifluktionen- und Frostmustererscheinungen im
17 Westteil Hochasiens, *Erlanger Geogr. Arb.*, 60, 150pp, 1998.
- 18 Gerlitz, L., Bechtel, B., Zaksek, K., Kawohl, T., and Böhner, J.: SAGA GIS based processing of
19 spatial high resolution temperature data, *Proceedings of the 27th EnviroInfo-Conference 2013*, 693-
20 702, 2013.
- 21 Gerlitz, L., Conrad, O., Thomas, A. and Böhner, J.: Assessment of Warming Patterns for the Tibetan
22 Plateau and its adjacent Lowlands based on an elevation- and bias corrected ERA-Interim Data Set,
23 *Climate Res.*, 58, 235-246, doi 10.3354/cr01193, 2014.
- 24 Giese, E.: Wetterwirksamkeit atmosphärischer Zustände und Prozesse in Sowjet-Mittelasien,
25 *Westfälische Geogr. Stud.*, 37, 395 – 410, 1973.
- 26 Giese, E.: Seßhaftwerden von Nomaden. Erfahrungen über die Dynamik traditioneller sozialer
27 Einrichtungen (am Beispiel des kasachischen Volkes), in: *Die Nomaden in Geschichte und*
28 *Gegenwart. Beiträge zu einem internationalen Nomadismus-Symposium am 11. und 12. Dezember*
29 *1975 im Museum für Völkerkunde Leipzig*, Berlin, 175-197, 1981.
- 30 Giese, E.: Nomaden in Kasachstan – Ihre Seßhaftwerdung und Einordnung in das Kolchos- und
31 Sowchossystem, *Geogr. Rundschau*, 11, 575 – 588, 1983.
- 32 Haase, G., Richer, H., and Barthel, H.: Zum Problem landschaftsökologischer Gliederung, dargestellt
33 am Beispiel des Changai-Gebirges in der Mongolischen Volksrepublik, *Wiss. Veröff. Deutschen Inst.*
34 *Länderk.*, 21/22, 489-516, 1964.

- 1 Hansen, M. C., Potapov, P. V., Moore, R., Hancher, M., Turubanova, S. A., Tyukavina, A., Thau, D.,
2 Stehman, S. V., Goetz, S. J., Loveland, T. R., Kommareddy, A., Egorov, A., Chini, L., Justice, C. O.,
3 and Townshend, J. R. G.: High-Resolution Global Maps of 21st-Century Forest Cover Change,
4 *Science*, 342, 850-853, doi 10.1126/science.1244693, 2013.
- 5 Hilbig, W.: *The Vegetation of Mongolia*, Amsterdam, 258pp, 1995.
- 6 Holdridge, L. R.: Determination of world plant formations from simple climatic data, *Science*, 105
7 (2727), 367–368, 1947.
- 8 Holtmeier, F.-K.: Die Höhengrenze der Gebirgswälder, *Arb. Inst. Landschaftsökologie*, 8, 337pp,
9 2000.
- 10 Hövermann, J.: Das System der klimatischen Geomorphologie auf landschaftskundlicher Grundlage,
11 *Z. Geomorphol. N.F., Supp.*, 56, 143-153, 1985.
- 12 Humboldt, A. von: *Kosmos: Entwurf einer physischen Weltbeschreibung*, Stuttgart, 5 volumes, 1847-
13 1862.
- 14 Jobbagy, E. G. and Jackson, R. B.: Global controls of forest line elevation in the northern and southern
15 hemispheres, *Global Ecol. and Biogeogr.*, 9, 253–268, 2000.
- 16 Kalnay, E., Kanamitsu, M., Kistler, R., Collins, W., Deaven, D., Gandin, L., Iredell, M., Saha, S.,
17 White, G., Woollen, J., Zhu, Y., Leetmaa, A., Reynolds, R., Chelliah, M., Ebisuzaki, W., Higgins, W.,
18 Janowiak, J., Mo, K. C., Ropelewski, C., Wang, J., Jenne, R., and Joseph, D.: The NCEP/NCAR 40-
19 year reanalysis project, *Bull. Amer. Meteor. Soc.*, 77, 437-470, 1996.
- 20 Karger, A.: Historisch-geographische Wandlungen der Weidewirtschaft in den Trockengebieten der
21 Sowjetunion am Beispiel Kasachstans, in: Knapp, R. (Edts.): *Weide-Wirtschaft in Trockengebieten*,
22 Gießen, 37-49, 1965.
- 23 Kastner, M.: Patterns of forest distribution in Western Mongolia, *Berliner Geowissensch. Abh.*, A 205,
24 67–71, 2000.
- 25 Klinge, M., Böhner, J., and Lehmkuhl, F.: Climate patterns, snow- and timberlines in the Altai
26 Mountains, Central Asia, *Erdkunde*, 57, 296-308, 2003.
- 27 Körner, C.: *Alpine Treelines, Functional Ecology of the Global High Elevation Tree Limits*, Springer,
28 Basel, 220 pp, 2012.
- 29 Körner, C. and Paulsen, J.: A world-wide study of high altitude treeline temperatures, *J. Biogeogr.*, 31,
30 713 – 732, 2004.
- 31 Liu, H., Williams, A. P., Allen, C. D., Guo, D., Wu, X., Anenkhonov, O. A., Liang, E., Sandanov, D.
32 V., Yin, Y., Qi, Z., and Badmaeva, N. K.: Rapid warming accelerates tree growth decline in semi-arid
33 forests of Inner Asia, *Glob. Change Biol.*, 19, 2500–2510, doi 10.1111/gcb.12217, 2013.

- 1 Lydolph, P. E.: *Climates of the Soviet Union*, World Survey of Climatology, 7, Amsterdam, 443pp,
2 1977.
- 3 Machalet, B., Frechen, M., Hambach, U., Oches, E. A., Zöllner, L., and Markovic, S. B.: The loess
4 sequence from Remisowka (northern boundary of the Tien Shan Mountains, Kazakhstan) -Part I:
5 Luminescence dating, *Quatern. Int.*, 152-153, 192-201, doi 10.1016/j.quaint.2005.12.014, 2006.
- 6 Mayer, T. and Bussemer, S.: *Die Waldsteppe Südsibiriens. Ökosystemanalyse mit Hilfe der*
7 *Radarfernerkundung*, Mitt. Geogr. Gesell. München, 85, 161-180, 2001.
- 8 Medeu, A. R.: *The national atlas of the Republic of Kazakhstan / Institute of Geography. Part 1:*
9 *Natural conditions and resources*, Almaty, 2010, 150pp, 2010.
- 10 Miehe, G. and Miehe, S.: Comparative high mountain research on the treeline ecotone under human
11 impact, *Erdkunde*, 54, 34–50, 2000.
- 12 Miehe, G., Miehe, S., Koch, K., and Will, M.: Sacred Forests in Tibet - Using Geographical
13 Information Systems for Forest Rehabilitation, *Mt. Res. Dev.*, 23/4, 324–328, 2003.
- 14 Miehe, G., Miehe, S., Will, M., Opgenoorth, L., Duo, L., Dorgeh, T., and Liu, J.: An inventory of
15 forest relicts in the pastures of Southern Tibet (Xizang A.R., China), *Plant Ecol.*, 194, 157–177 doi
16 10.1007/s11258-007-9282-0, 2008.
- 17 Paulsen, J. and Körner, C.: A climate-based model to predict potential treeline position around the
18 globe, *Alpine Botany*, 124, 1–12, doi 10.1007/s00035-014-0124-0, 2014.
- 19 Rabus, B., Eineder, M., Roth, A., and Bamler, R.: The shuttle radar topography mission -a new class of
20 digital elevation models acquired by spaceborne radar, *ISPRS J. Photogramm.*, 57, 241–262, 2003.
- 21 Schlütz, F., Dulamsuren, C., Wieckowska, M., Mühlenberg, M., and Hauck, M.: Late Holocene
22 vegetation history suggests natural origin of steppes in the northern Mongolian mountain taiga,
23 *Palaeogeogr. Palaeoclimatol.*, 261, 203–217, 2008.
- 24 Soria-Auza, R.W., Kessler, M., Bach, K., Barajas-Barbosa, P.M., Lehnert, M., Herzog, S.K., and
25 Böhner, J.: Impact of the quality of climate models for modelling species occurrences in countries
26 with poor climatic documentation: a case study from Bolivia, *Ecol. Model.*, doi
27 10.1016/j.ecolmodel.2010.01.004, 2010.
- 28 Treter, U.: Gebirgs-Waldsteppe in der Mongolei, *Geogr. Rundschau*, 48/11, 655-661, 1996.
- 29 Treter, U.: Recent extension and regeneration of the larch forest in the mountain forest steppe of north-
30 west Mongolia, *Marburger Geogr. Schriften*, 135, 156-170, 2000.
- 31 Troll, C.: The upper timberlines in different climate zones, *Arctic Alpine Res.*, 5, A3-A18, 1973a.
- 32 Troll, C.: High mountain belts between the polar caps and the equator: Their definition and lower
33 limit, *Arctic Alpine Res.*, 5, A19-A27, 1973b.

- 1 Walter, H. and Breckle, S.W.: Spezielle Ökologie der Gemäßigten und Arktischen Zonen Euro-
- 2 Nordasiens, Ökologie der Erde, 3, Jena, 726pp, 1994.
- 3 Wang, T., Ren, H., and Ma, K.: Climatic signals in tree ring of *Picea schrenkiana* along an altitudinal
- 4 gradient in the central Tianshan Mountains, northwestern China, *Trees*, 19, 735–741, doi
- 5 10.1007/s00468-005-0003-9, 2005.
- 6 Wang, T., Zhang, QB., and Ma, K.: Treeline dynamics in relation to climatic variability in the central
- 7 Tianshan Mountains, northwestern China, *Global Ecol. and Biogeogr.*, 15, 406–415, 2006.

1 **Table 1:** Confusion matrix showing the accuracy report of the supervised maximum likelihood
 2 classification (area in ha)

		Classification data		Sum reference	Producer's accuracy	Omission error
		Forest	No forest			
Reference data	Forest	2,696.7	333.6	3,030.3	0.890	0.110
	No forest	14.7	76,426.2	76,440.9	0.9998	
Sum classification		2,711.4	76,759.8	Total Sum of test data	Overall accuracy	
User's accuracy		0.995	0.995			
Commission error		0.0054		79,471.2	0.996	

1 **Table 2:** Statistical values of the relief parameters related to the forest distribution.

Parameter	Unit	Maximum distribution value	Total distribution range	95% of the distribution range
Elevation	m asl.	2500	1575 - 2900	1925 - 2775
Aspect	degree horizontal	315 (NW)	0 - 360	260 - 70
Slope gradient	degree vertical	28	0 - 62	12 - 38
Solar radiation input	kWh/m ²	1075	450 - 1550	800 - 1325

2

3

1 **Table 3:** Comparison between of the modelled area values of single relief parameter classes and of the
 2 combination of all four relief parameters. (AFA = Actual forest area, PFA = Potential forest area)

Relief parameter : Site classification	Elevation			Solar radiation input			Slope gradient			Slope aspect			All 4 parameters		
	km ²	% FA _{AP}	% TMA	km ²	% FA _{AP}	% TMA	km ²	% FA _{AP}	% TMA	km ²	% FA _{AP}	% TMA	km ²	% FA _{AP}	% TMA
3.) PFA without AFA	5358.7	91.4	65.9	4791.2	90.5	59.0	4279.9	89.5	52.7	3850.5	88.5	47.4	1323.6	72.5	16.3
1.) PFA with AFA	502.0	8.6	6.2	480.5	9.1	5.9	483.8	10.1	6.0	474.2	10.9	5.8	446.7	24.5	5.5
4.) No PFA with AFA	0.3	0.004	0.003	21.5	0.4	0.3	18.0	0.4	0.2	27.9	0.6	0.3	55.4	3.0	0.7
2.) No PFA without AFA	2265.2		27.9	2832.9		34.9	3344.4		41.2	3773.6		46.4	6300.7		77.5
Sum of all classifications which represent the actual situation	2767.2		34.1	3313.4		40.8	3828.3		47.1	4247.8		52.3	6747.4		83.0

% FA_{AP} = Percent portion of the total actual and potential forest area

% TMA = Percent portion of total mountain area with 8126 km²

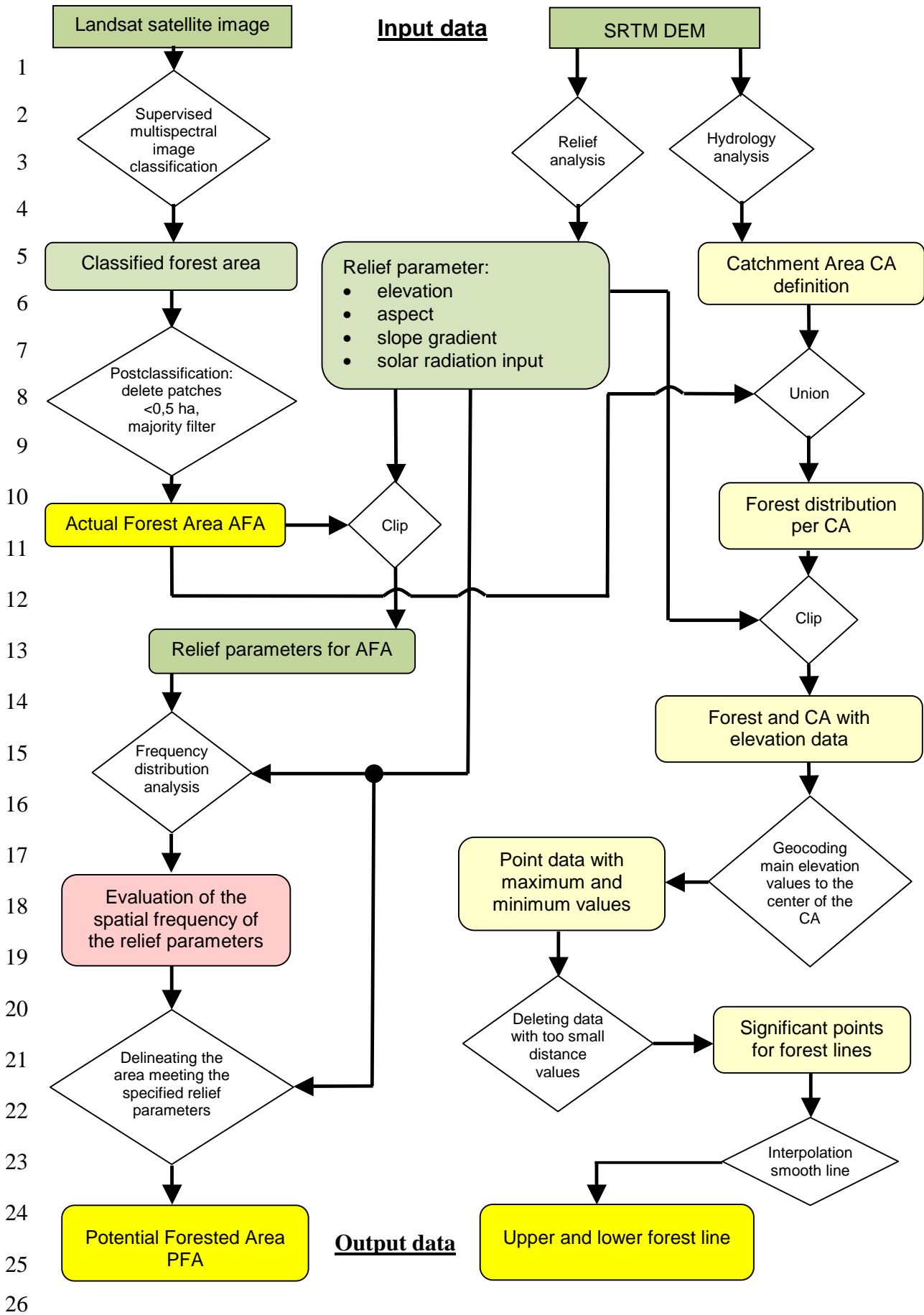
3



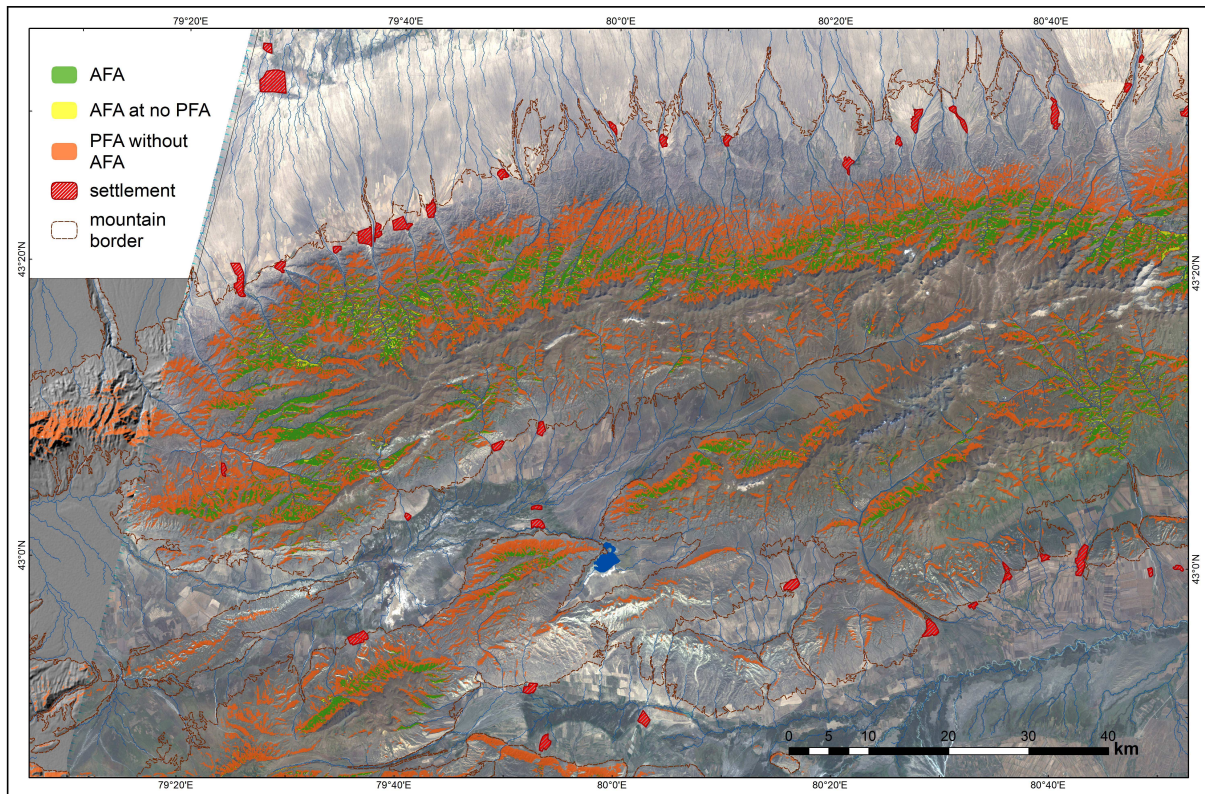
1

2 **Figure 1:** Map overview showing the detailed investigation area (rectangle) in Central Asia

3

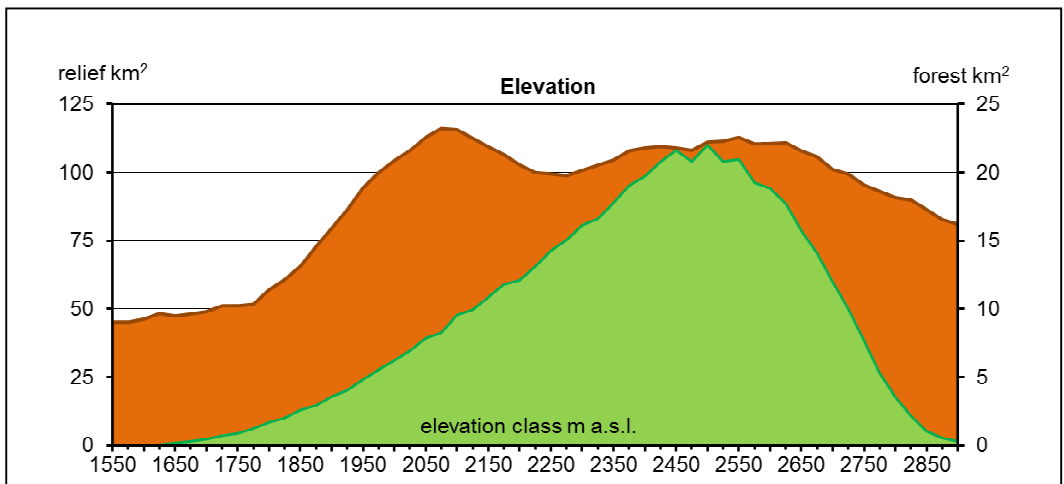


27 **Figure 2:** Workflow of DEM and satellite image processing to determine the spatial forest
 28 distribution patterns in semi-arid Mountain systems of Central Asia in a high resolution scale.

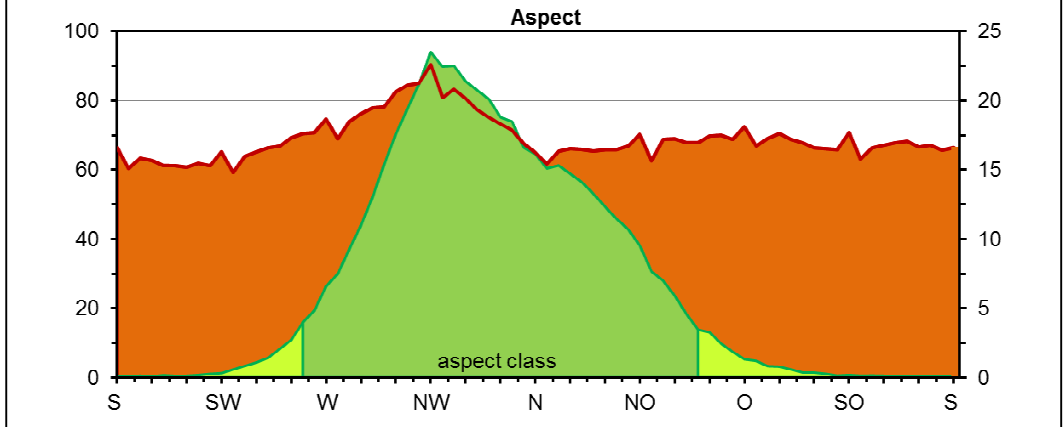


1
 2 **Figure 3:** Spatial distribution of actual forested area AFA and potential forest area PFA in the
 3 mountainous region of northernmost Tien Shan shown above a true colour composite of a
 4 Landsat 7 satellite image of the 13th September 2000.

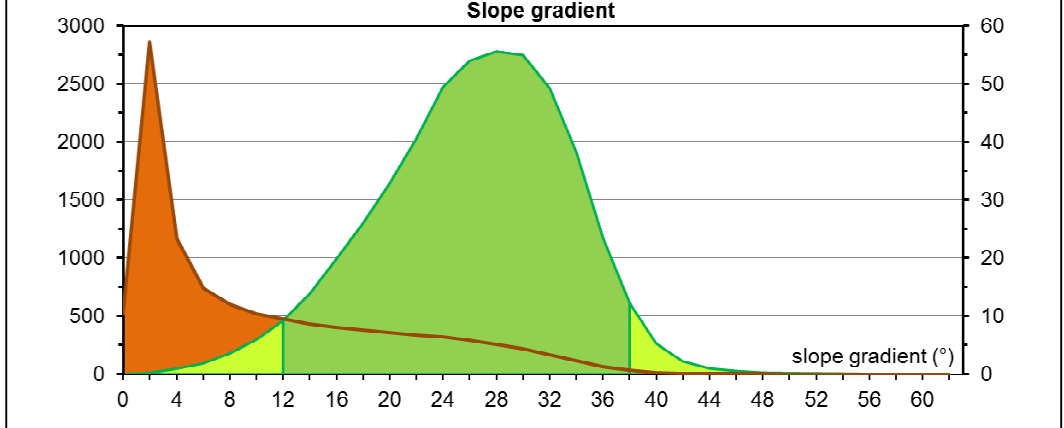
1



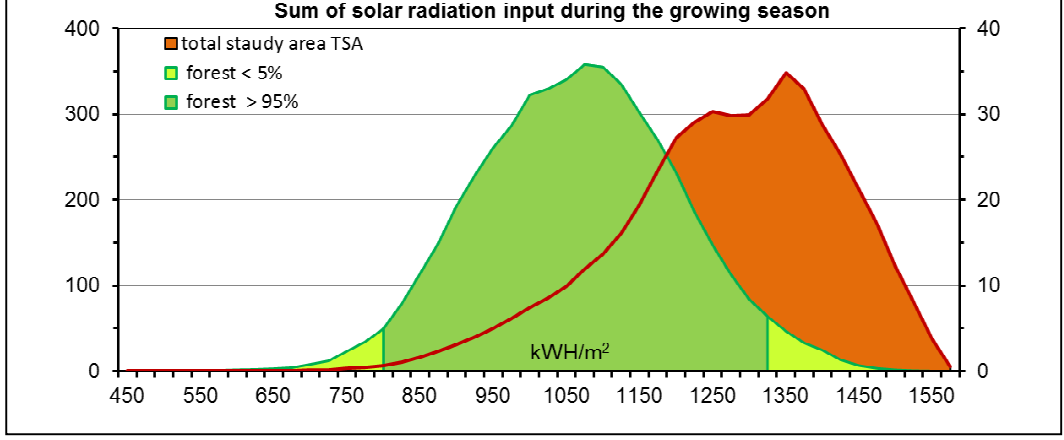
2



3

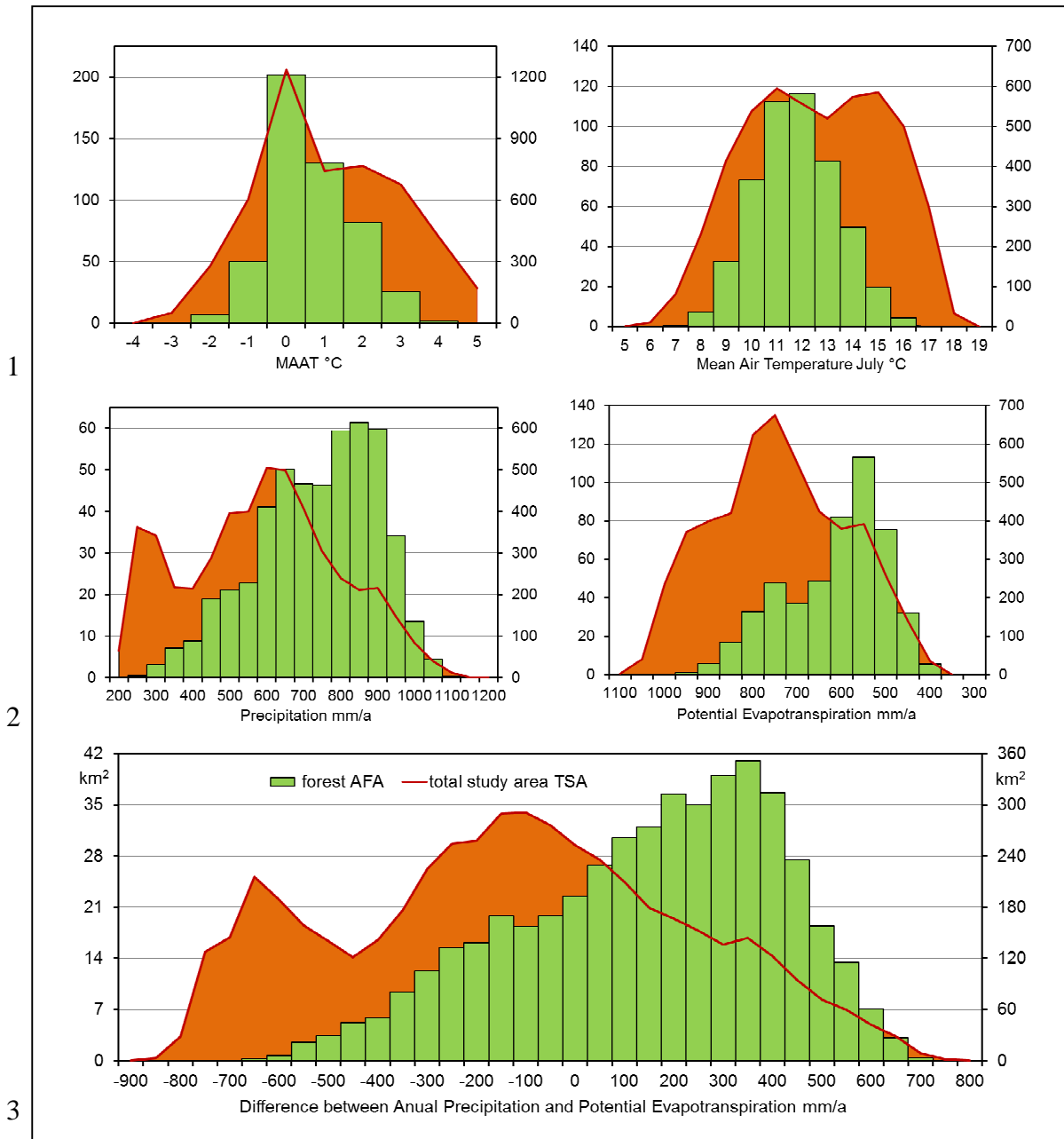


4

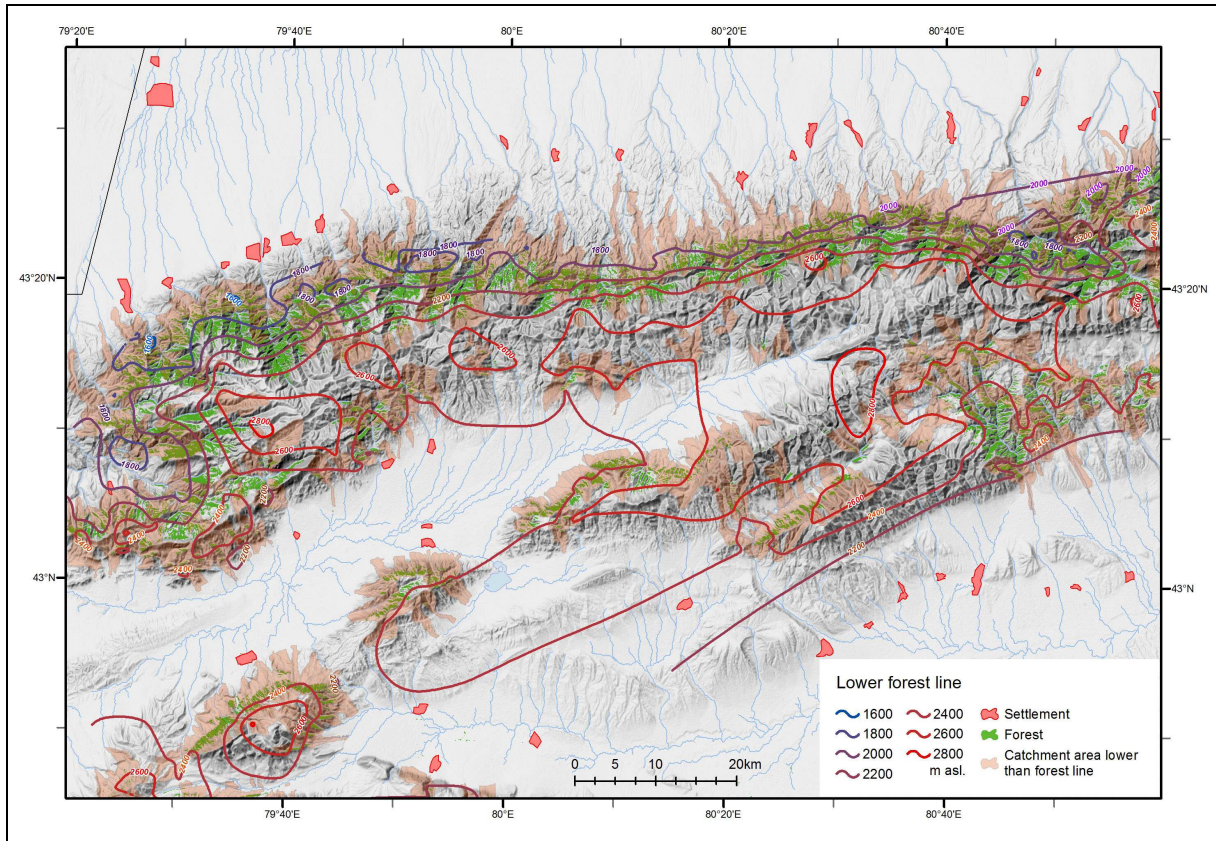


5

6 **Figure 4:** Frequency distribution of relief parameters in relation to actual forest area AFA (for
 7 the diagrams aspect, slope gradient, and solar radiation input: dark green = standard deviation
 8 95%, light green = marginal value range excluded from PFA delineation) and total study area
 9 (TSA, brown).

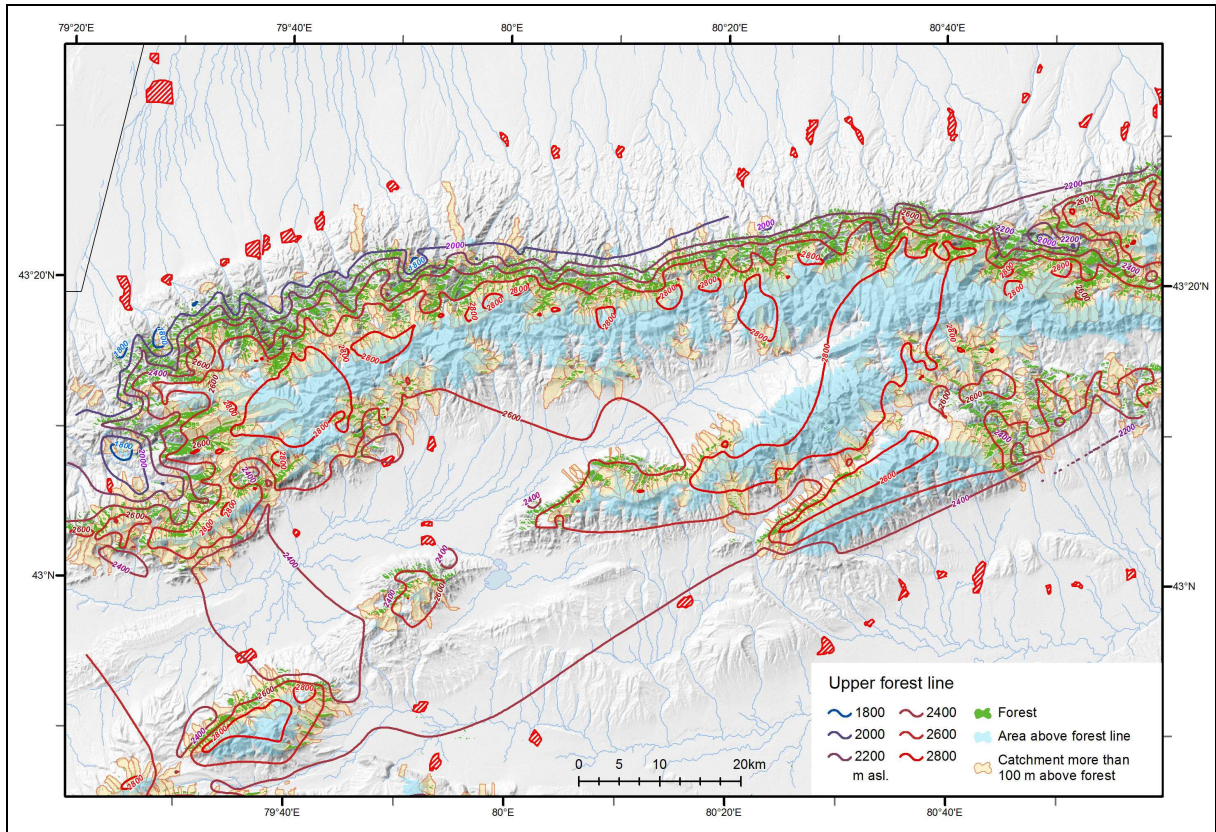


4 **Figure 5:** Frequency distribution of climate parameters for actual forest area (AFA, columns,
5 left axes km²) and the total study area (TSA, graph, right axes km²).



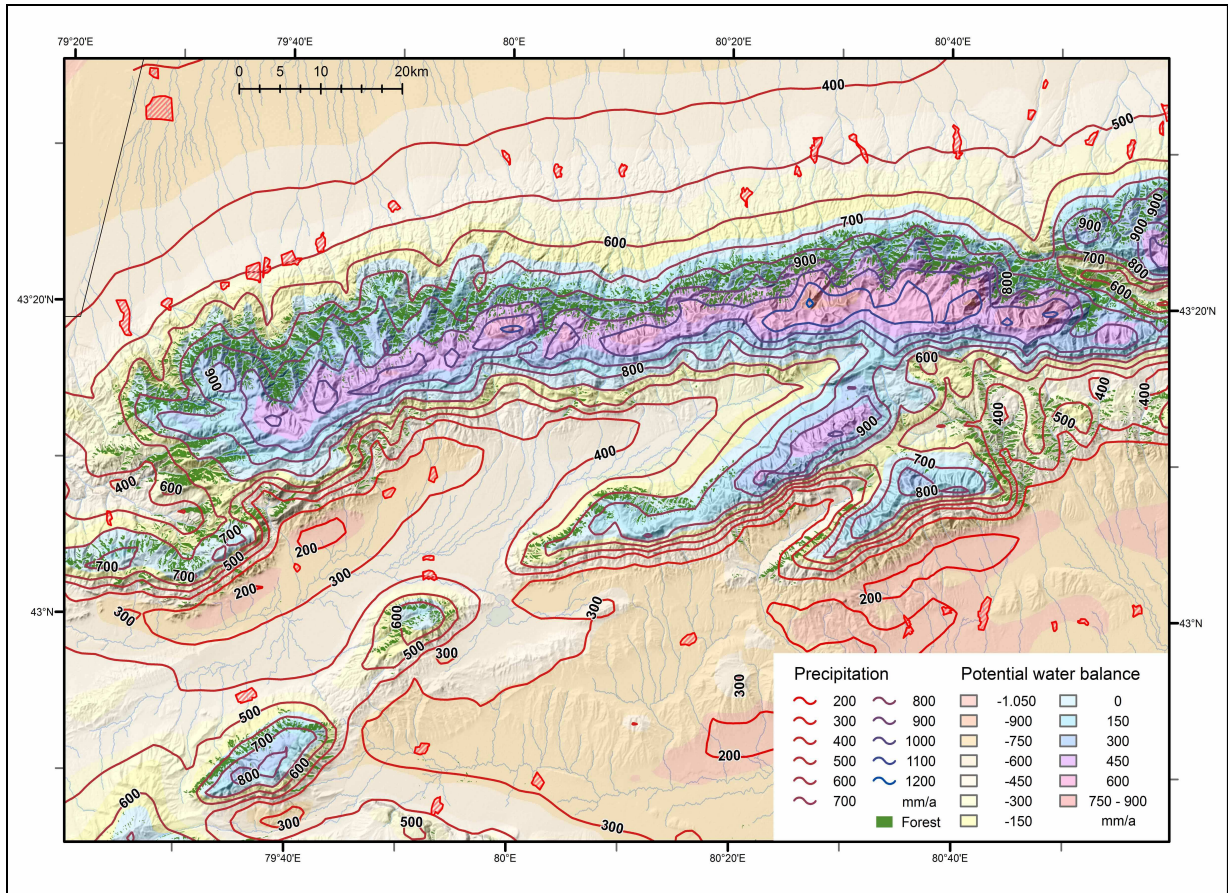
1

2 **Figure 6:** The lower forest line and the catchment areas providing lower forest line values in
 3 the investigation area.



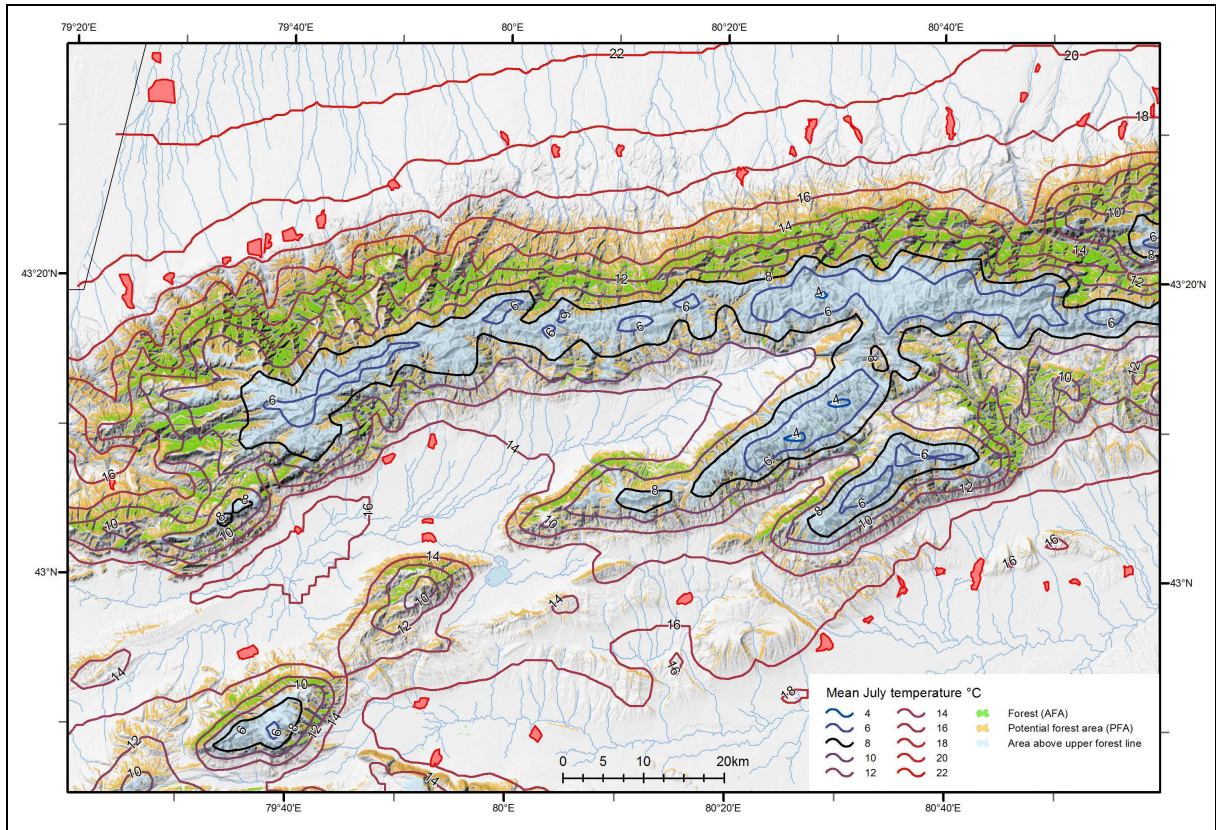
1

2 **Figure 7:** The upper forest line and the catchment areas providing upper forest line values in
 3 the investigation area.



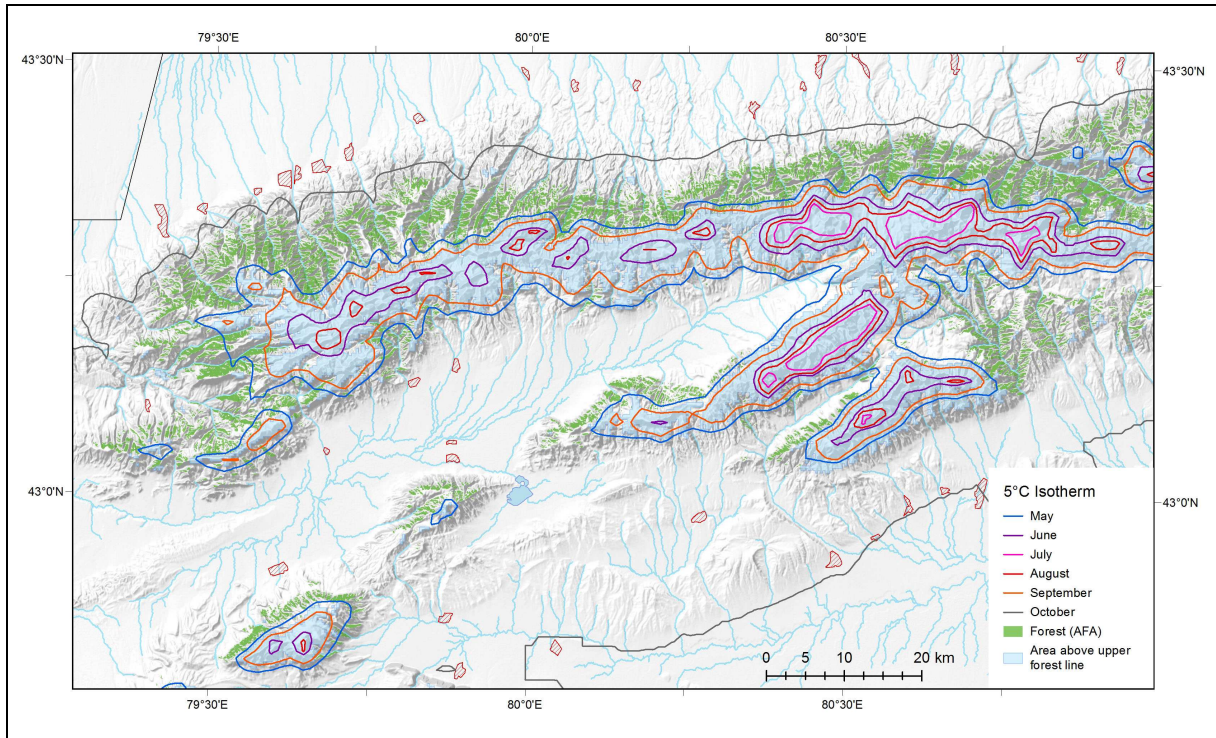
1

2 **Figure 8:** Forest distribution AFA in relation to the hydrological climatic environment



1

2 **Figure 9:** Forest distribution AFA and PFA and the July isotherms.



1

2 **Figure 10:** Forest distribution AFA and the 5 °C monthly isotherms during the growing
 3 season.